Article

Cobalt (II) Complexes with Schiff Base Ligands Derived from Terephthalaldehyde and *ortho*-Substituted Anilines: Synthesis, Characterization and Antibacterial Activity

Sahar Shaygan, Hoda Pasdar *, Naser Foroughifar, Mehran Davallo and Fereshteh Motiee

Department of Chemistry, North Tehran Branch, Islamic Azad University, Tehran 1651153311, Iran; shrshaigan@yahoo.com (S.S.); n_foroughifar@yahoo.com (N.F.); m_davallo@yahoo.com (M.D.); f_motiee@iau-tnb.ac.ir (F.M.)
* Correspondence: h_pasdar@iau-tnb.ac.ir; Tel./Fax: +98-212-222-2512

Abstract: In this study, *N*-propyl-benzoguanamine-SO_3H magnetic nanoparticles (MNPs) were used as a catalyst for the synthesis of new Schiff base ligands from condensation reaction of terephthalaldehyde and *ortho*-aniline derivatives. The bioactive ligands and their cobalt (II) complexes were characterized with nuclear magnetic resonance (^{1}H-NMR), Fourier-transform infrared spectroscopy (FT-IR), ultraviolet-visible (UV-Visible), mass spectroscopy studies and molar conductance. The antibacterial activity of ligands and their metal complexes were screened using disc diffusion and broth dilution methods against *Escherichia coli*, *Serratia marcescens*, *Pseudomonas aeruginosa* (gram negative bacteria), *Bacillus Subtilis* and *Staphylococcus aureus* (gram positive bacteria). The ligands with hydroxyl group showed better biological activity when compared to other ligands. The results showed that the metal complexes have much higher antibacterial activity compare to the parent ligands. It was found that the CoL_3 complex was more effective than other metal complexes used against all types of bacteria tested and it was more effective against *Pseudomonas aeruginosa* with diameter inhibition zone of 17 mm and minimal inhibitory concentration value of 0.15 mg/mL.

Keywords: terephthalaldehyde; *ortho*-aniline derivatives; Schiff base ligand; antibacterial activity; disc diffusion method; broth dilution method

1. Introduction

Schiff base ligands with oxygen or nitrogen donor atoms are a good class of organic compounds capable of binding to different metal ions with interesting medical and non-medical properties and very popular in the last decade [1,2]. These ligands can be easily synthesized by condensation reaction of aldehyde or ketone with a primary amine [3]. The multifarious role of transition complexes of Schiff base ligands in inorganic, metallo-organic and biochemistry have received considerable attention because of their extensive applications in a wide range of areas [4,5].

They display diverse chemical, optical and magnetic properties by modifying with different ligands [6–8]. It has been revealed that Schiff bases play an important role by serving as chelating ligands in the main groups and transition metal coordination chemistry; owing to their stability in different oxidative and reductive conditions [9]. The interaction of these donor ligands and metal ions gives complexes of different geometries and literature survey reveals that these complexes are potentially more biologically active compounds [10] such as anticancer, antifungal, antibacterial, antimalarial, anti-inflammatory, antiviral, and antipyretic properties [11–14]. It should be noted that

metal chelation can tremendously influence the antimicrobial/bioactive behavior of the organic ligands; therefore, the synthesis of various transition metal complexes has been attempted in this field [15].

In the past few years, bacterial infection and their resistance for many antibacterial agents is a growing problem [16,17]. While there are already several classes of antibacterial agents, there has been some considerable emerging resistance in most pathogenic bacteria to these drugs [18]. For prevention of this serious medical problem, it is necessary to develop some new antibacterial agents or to expand the bioactivity of the previously used drugs [19,20]. Metal-based antibacterial compounds seem to be a promising research for designing a novel therapeutic methodology for new antibiotic drugs to control and prevent the growth of bacterial strains [21,22].

Herein, we report the synthesis of bidentate Schiff base ligands by the condensation of terephthalaldehyde with *ortho*-aniline derivatives in the presence of *N*-propyl-benzoguanamine-SO$_3$H MNPs as a catalyst. The cobalt (II) complexes were prepared in methanol as a solvent. The synthesized compounds were characterized with several spectroscopic methods and screened for their antibacterial activity against Gram (+) and Gram (−) bacteria strains.

2. Materials and Methods

2.1. Materials

All the chemicals and solvents purchased from Merck (Darmstadt, Germany) and Sigma-Aldrich Company (St. Louis, MO, USA) and were used without further purification unless otherwise mentioned. UV-Vis (see Supplementary Materials) absorption spectra were recorded on a Cary 100 spectrophotometer (Santa Clara, CA, USA) using a 1 cm path length cell. 1H-NMR (see Supplementary Materials) spectra of ligands were collected on BRUKER 250 MHz spectrometer (Seiko, Japan) in DMSO-d_6 using tetramethylsilane as internal standard. The Fourier-transform infrared spectroscopy (FTIR) spectra (see Supplementary Materials) (KBr pellets) were recorded using a Shimidzo 300 spectrometer. Melting points of compounds were obtained by an electro thermal melting point apparatus and were not corrected. Thin-Layer chromatography (TLC) was performed using n-hexane/EtOAC (1:3) as an eluent.

2.2. Preparation of Schiff Base Ligands

Condensation reaction of Terephthalaldehyde with o-nitroaniline, o-Anisidine and 2-aminophenol in molar ratio 1:1 and 1:2 afforded the corresponding Schiff base ligands as described below:

MNPS-*N*-propyl-benzoguanamine-SO$_3$H catalyst was prepared by chemical co-precipitation according to the previous literature [23]. To a mixture of terephthalaldehyde and aniline derivative was added to *N*-propyl-benzoguanamine-SO$_3$H catalyst (6 mg) in 10 mL ethanol as solvent. The reaction mixture was refluxed (100 °C) for 2–3 h. The progress of the reaction was checked with TLC. After completion of the reaction the mixture was cooled to room temperature. The catalyst was then separated by using an external magnet. The solvent was evaporated under reduced pressure and the resulting solid was obtained. The resulting was then recrystallized in ethanol.

(1,4-phenylenebis(methanylylidene))bis(2-nitroaniline) (**L$_1$**): Dark Yellow solid. Yield: 84%. M.P. 208–210 °C. Selected IR data (ν, cm^{-1}): 2924, 1630, 1449, 1348, 1012. ^{1}H-NMR (500 MHz, DMSO-d_6, δ, ppm): 10.04 (s, 2H, CH=N), 8.02–7.97 (q, 12.5 Hz, 8H, Ar-H), 7.90–7.87 (d, 7.5 Hz, 2H, Ar-H), 7.53–7.50 (d, 7.5 Hz, 2H, Ar-H). UV-Vis (DMSO): λ$_{max}$ (nm) = 260, 340.

(1,4-phenylenebis(methanylylidene))bis(2-methoxyaniline) (**L$_2$**): Orange solid. Yield: 86%. M.P. 190–192 °C. Selected IR data (ν, cm^{-1}): 3062, 3018, 2965, 2835, 1620, 1116. ^{1}H-NMR (250 MHz, DMSO-d_6, δ, ppm): 10.08 (s, 2H, CH=N), 8.66–8.60 (m, 2H, Ar-H), 8.14–8.02 (m, 5H, Ar-H), 7.35–6.95 (m, 8H, Ar-H), 3.80 (s, 6H, CH$_3$). UV-Vis (DMSO): λ$_{max}$ (nm) = 290, 390.

(1,4-phenylenebis(methanylylidene))bis(azanylylidene))diphenol (**L$_3$**): Brown solid . Yield: 64%. M.P. 295–297 °C. Selected IR data (ν, cm^{-1}): 3412, 3100, 1614, 1059. ^{1}H-NMR (500 MHz, DMSO-d_6, δ,

ppm): 9.72 (s, 2H, CH=N), 8.34–8.32 (d, 5Hz, 2H, Ar-H), 8.19–8.17 (d, 5Hz, 2H, Ar-H), 7.86–7.82 (m, 2H, Ar-H), 7.67–7.66 (d, 2.5 Hz, 1H, Ar-H), 7.48–7.42 (m, 2H, Ar-H), 7.07–7.03(m, 2, OH). UV-Vis (DMSO): λ_{max} (nm) = 330.

4-(((2-nitrophenyl)imino)methyl)benzaldehyde (**L₄**): Yellow solid. Yield: 68%. M.P. 203–205 °C. Selected IR data (ν, cm^{-1}): 2948, 2900, 1702, 1619, 1568, 1356, 1073. ^{1}H-NMR (250 MHz, CDCl$_3$, δ, ppm): 10.99 (s, 1H, CHO), 10.06 (s, 1H, CH=N), 8.16–8.02 (m, 5H, Ar-H), 7.79–7.69 (m, 3H, Ar-H). UV-Vis (DMSO): λ_{max} (nm) = 250, 320.

4-(((2-methoxyphenyl)imino)methyl)benzaldehyde (**L₅**): Pale Yellow solid. Yield: 73%. M.P. 181–183 °C. Selected IR data (ν, cm^{-1}): 3011, 2966, 2838, 1693, 1620, 1102. ^{1}H-NMR (500 MHz, DMSO-d_6, δ, ppm): 10.07 (s, 1H, CHO), 8.64 (s, 1H, CH=N), 8.03–8.01 (d, 5 Hz, 4H, Ar-H), 7.21–6.95 (m, 4H, Ar-H), 3.79 (s, 6H, CH$_3$). UV-Vis (DMSO): λ_{max} (nm) = 290, 370.

4-(((2-hydroxyphenyl)imino)methyl)benzaldehyde (**L₆**): Light Green solid. Yield: 65%. M.P. 282–284 °C Selected IR data (ν, cm^{-1}): 3431, 3147, 3046, 1703, 1652, 1028. ^{1}H-NMR (500 MHz, DMSO-d_6, δ, ppm): 10.18 (s, 1H, CHO), 9.73 (s, 1H, CH=N), 8.41–7.45 (m, 8H, Ar-H), 1.21 (s, 1H, OH). UV-Vis (DMSO): λ_{max} (nm) = 320.

2.3. Preparation of Co (II) Complexes

All the complexes were prepared in a similar procedure. Solution of ligand in methanol (1 mmol) were mixed with CoCl$_2$·6H$_2$O and refluxed for 3–5 h 45 °C. The precipitate was filtered, washed with methanol and ether and then dried in a vacuum desiccator.

Complex [Co₂(1,4-phenylenebis(methanylylidene))bis(2-nitroaniline)Cl₄] (**CoL₁**): Pale Green solid. Yield: 84%. M.P. 248–250 °C. Molar conductivity (Ω^{-1} mol^{-1} cm^2): 22. Selected IR data (ν, cm^{-1}): 3109, 2971, 1651, 1521, 1384, 598, 492. UV-Vis (DMSO): λ_{max} (nm) = 300, 410, 600,690. Mass (see Supplementary Materials): $[m/z]^+$ = 633.

Complex [Co₂(1,4-phenylenebis(methanylylidene))bis(2-methoxyaniline)Cl₄] (**CoL₂**): Dark Green solid. Yield: 68%. M.P. 313–315 °C. Molar conductivity (Ω^{-1} mol^{-1} cm^2): 12. Selected IR data (ν, cm^{-1}): 3062, 3018, 1620, 1583, 1368, 511, 474. UV-Vis (DMSO): λ_{max} (nm) = 290, 260, 610, 690, 750. Mass: $[m/z]^+$ = 603.

Complex [Co₂(1,4-phenylenebis(methanylylidene))bis(azanylylidene))diphenol)Cl₄] (**CoL₃**): Dark Brown solid. Yield: 75%. M.P. 230–232 °C. Molar conductivity (Ω^{-1} mol^{-1} cm^2): 14. Selected IR data (ν, cm^{-1}): 3100, 2841, 1650, 537, 485. UV-Vis (DMSO): λ_{max} (nm) = 280, 370, 600, 680. Mass: $[m/z]^+$ = 575.

Complex [Co(4-(((2-nitrophenyl)imino)methyl)benzaldehyde)Cl₂] (**CoL₄**): Green solid. Yield: 80%. M.P. 280–282 °C. Molar conductivity (Ω^{-1} mol^{-1} cm^2): 8. Selected IR data (ν, cm^{-1}): 3181, 1599, 614. UV-Vis (DMSO): λ_{max} (nm) = 320, 600,690. Mass: $[m/z]^+$ = 503.

Complex [Co(4-(((2-methoxyphenyl)imino)methyl)benzaldehyde)Cl₂] (**CoL₅**): Orange-Red solid. Yield: 82%. M.P. 305–307 °C. Molar conductivity (Ω^{-1} mol^{-1} cm^2): 16. Selected IR data (ν, cm^{-1}): 3100, 2900, 1619, 568, 509. UV-Vis (DMSO): λ_{max} (nm) = 290, 370, 600, 670. Mass: $[m/z]^+$ = 473.

Complex [Co(4-(((2-hydroxyphenyl)imino)methyl)benzaldehyde)Cl₂] (**CoL₆**): Dark Pink solid. Yield: 87%. M.P. 236–238 °C. Molar conductivity (Ω^{-1} mol^{-1} cm^2): 10. Selected IR data (ν, cm^{-1}): 2959, 1634, 649. UV-Vis (DMSO): λ_{max} (nm) = 270, 350, 610, 670. Mass: $[m/z]^+$ = 445.

2.4. Antibacterial Study

All the synthesized compounds were evaluated to examine their in vitro antibacterial activities against *Escherichia coli* (ATCC: 25922), *Serratia marcescens* (ATCC: 13880) and *Pseudomonas aeruginosa* (ATCC: 27853) as gram negative bacteria and *Bacillus subtilis* (ATCC: 6633), and *Staphylococcus aureus* (ATCC: 6838), as gram positive bacteria, by employing two methods: disk diffusion and broth dilution methods; which are recommended by the National Committee for Clinical Laboratory Standards (NCCLS) [24].

Accordingly, stock solution of each compound (2 mg/mL) was prepared by dissolving the compounds in DMSO. Prior to sensitivity testing, the bacteria strains were cultured onto Muller-Hinton agar plate and incubated for 18–24 h at 35 °C. The density of the bacteria culture required for the tests was adjusted to 0.5 McFarland (1.5×10^8 CFU/mL) (CFU = Colony Forming Unit). These tests were repeated three times to ensure reliability.

2.4.1. Disc Diffusion Method

This method is based on the principles that an antibiotic-impregnated disk placed on an agar previously inoculated with the test bacterium, the pick-up moisture and the antibiotic diffused radially outward through the agar medium, yielding an antibiotic concentration gradient. For this purpose, 2 mg of the synthesized compound was dissolved in 1 mL DMSO. A bacteria culture was swabbed uniformly across lawn Hinton agar plates. Paper discs were impregnated individually with 100 µL of stock solution of the compounds. Next, the discs were placed on the inoculated agar medium and the plates incubated for 18–24 h at 35 °C. After the incubation time, antibacterial activity of each sample was determined by measuring the inhibition zone around each disc by comparing it with the standard drug (Tetracycline).

2.4.2. Broth Dilution Method

Minimal Inhibitory Concentration (MIC) value of an antibacterial agent gives a quantitative estimate of the susceptibility for each bacteria strain. MIC is defined as the lowest concentration of the antimicrobial agent which is required to inhibit the growth of the microorganism. According to this method, 1 mL of sterile Muller Hinton Broth medium were poured in tube 1–13 with two-fold dilutions of the synthesized compound (2 to 0.00195 mg/mL) and inoculated with a standardized inoculum of the bacteria (1.5×10^8); then it was incubated under standardized conditions by following NCCLS guidelines. After 18–24 h of incubation at 35 °C, the MIC value was recorded as the lowest concentration of antimicrobial agent with no visible growth.

3. Results and Discussion

3.1. Characterization of Ligands

Six Schiff base Ligands (**L₁–L₆**) were synthesized by condensation reaction of terephthaldehyde and o-aniline derivatives in the presence of *N*-propyl-benzoguanamine-SO₃H MNPs under optimized condition. The magnetic nanoparticles were prepared according to the previous literature [23]. The method for the synthesis of Schiff base ligands is given in Figure 1. In order to optimize the reaction condition of starting materials, the reaction of terephthaldehyde (1 mmol) and o-nitroaniline (2 mmol) was carried out in different conditions using different solvents and catalysts with different catalyst content.
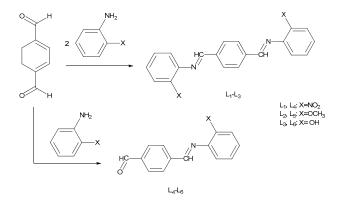

Figure 1. The method for synthesis of Schiff base ligands.

According to Table 1 the type of solvent and amount of catalyst was observed to have a significant effect on the yield of reaction using similar catalyst (*N*-propyl-benzoguanamine-SO$_3$H MNPs). The highest yield was obtained up to 84%with a shorter reaction time using ethanol as solvent. In the next step, the amount of catalyst in the reaction was also examined. It is obvious from Table 1 that applying more than the specified quantity of catalyst did not have a positive effect on the yield of product and 6 mg of the catalyst represented the best yield of the reaction. It is noted from Table 1, with increasing the amount of catalyst from 3 mg to 11 mg, reaction yield was reduced 25% with a longer reaction time. The effect of p-Toluenesulfonic acid (PTSA) as catalyst was further examined which exhibited lower reaction yield with much longer reaction time.

Table 1. Optimization of reaction condition for synthesis of (**L$_1$**–**L$_6$**) ligands. MNPs: magnetic nanoparticles; PTSA: p-Toluenesulfonic acid.

Entry	Catalyst (mg)	Solvent	Time (min)	Yield (%)
1	MNPs-*N*-propyl-benzoguanamine-SO$_3$H (3)	H$_2$O	300	45
2	MNPs-*N*-propyl-benzoguanamine-SO$_3$H (3)	EtOH:H$_2$O	210	53
3	MNPs-*N*-propyl-benzoguanamine-SO$_3$H (3)	EtOH	180	68
4	MNPs-*N*-propyl-benzoguanamine-SO$_3$H (6)	EtOH	120	84
5	MNPs-*N*-propyl-benzoguanamine-SO$_3$H (9)	EtOH	210	75
6	MNPs-*N*-propyl-benzoguanamine-SO$_3$H (11)	EtOH	300	63
7	PTSA (6)	EtOH	480	35

The ligands were characterized by nuclear magnetic resonance (^{1}H-NMR), Fourier-transform infrared spectroscopy (FT-IR) and ultraviolet-visible (UV-Visible). In the ^{1}H-NMR spectra of the (**L$_1$**–**L$_6$**) ligand, the singlet peaks due to the CNH (azomethine) group were observed in the range of 10.08–8.64 ppm as singlet. Regarding the ^{1}H-NMR spectra of the compounds, it can be observed that the CNH signals of the Schiff base ligands shifted to a lower ppm (shielding) when electron donating (OH) substituent was used and it moved to a higher ppm (deshielding) when a withdrawing group (NO$_2$) was used. Condensation of amine groups to Terephthaldehyde in all of the ligands is confirmed by the absence of the N-H protons. The signals of the methyl groups (-CH$_3$) for **L$_2$** and **L$_5$**, and OH groups for **L$_3$** and **L$_6$** ligands are observed in the range of 3.80–3.79 ppm and 1.21–1.16 ppm, respectively. In the ^{1}H-NMR spectra of **L$_4$**, **L$_5$** and **L$_6$** ligands the CHO protons are seen at 10.99, 10.07 and 10.18 ppm, respectively. The aromatic protons of the Schiff base ligands are observed in the range of 8.66–6.82 ppm. The ^{1}H NMR spectral data of the ligands are summarized in Table 2.

Table 2. ^{1}H NMR spectral data of the ligands.

Compounds	HCN (ppm)	CHO (ppm)	Ar-H (ppm)	CH$_3$ (ppm)	OH (ppm)
L$_1$	10.04	-	8.02–7.50	-	-
L$_2$	10.08	-	8.66–6.95	3.80	-
L$_3$	9.72	-	8.34–6.82	-	1.16
L$_4$	10.06	10.99	8.16–7.69	-	-
L$_5$	8.64	10.07	8.03–6.95	3.79	-
L$_6$	9.73	10.18	8.41–7.45	-	1.21

The FTIR spectra of the ligands showed peaks in the range of 1652–1620 cm^{-1} assigned to ν(C=N). In the L$_4$, L$_5$ and L$_6$ the ν(C=O) (carbonyl) stretching appeared at 1702, 1693 and 1703 cm^{-1}, respectively. In **L$_1$** and **L$_4$** Schiff bases the bands observed in the range of 1568–1348 cm^{-1} are attributed to the NO$_2$ groups, while the OH groups of **L$_3$** and **L$_6$** appeared at 3553 and 3438 cm^{-1}, respectively.

The UV-Visible spectra of all the ligands and compounds are recorded in DMSO and the data are listed in Table 3. In the electronic spectra of **L$_1$**, **L$_2$**, **L$_4$** and **L$_5$** two peaks appeared which are attributed to π→π* and n→π* transitions, respectively. In **L$_3$** and **L$_6$** one intense absorption band

observed in 310 and 340 nm is due to the п→п* transition. However, п→п* and n→п* absorption peaks exhibited different behaviors due to the nature of substituents. In the UV-Vis spectra of the ligands with withdrawing group (NO_2) the п→п* peak shifted to a lower wavelengths (blue-shift) as compared to the ligands, whereas with electron donating group (OH) the п→п* peak observed in higher wavelengths (red-shift).

Table 3. Electronic spectra data for ligands and complexes.

Compounds	Band Position (nm)	Assignment
L_1	260	$\pi \rightarrow \pi^*$
	350	$n \rightarrow p^*$
L_2	300	$\pi \rightarrow \pi^*$
	390	$n \rightarrow p^*$
L_3	310	$\pi \rightarrow \pi^*$
L_4	290	$\pi \rightarrow \pi^*$
	320	$n \rightarrow p^*$
L_5	290	$\pi \rightarrow \pi^*$
	370	$n \rightarrow p^*$
L_6	340	$\pi \rightarrow \pi^*$
CoL_1	310	$\pi \rightarrow \pi^*$
	350	$n \rightarrow p^*$
	600	$^4A_1 \rightarrow {}^4B_1$
	690	$^4A_1 \rightarrow {}^4B_2$
CoL_2	280	$\pi \rightarrow \pi^*$
	410	$n \rightarrow p^*$
	610	$^4A_1 \rightarrow {}^4B_1$
	680	$^4A_1 \rightarrow {}^4B_2$
CoL_3	280	$\pi \rightarrow \pi^*$
	370	$n \rightarrow p^*$
	600	$^4A_1 \rightarrow {}^4B_1$
	680	$^4A_1 \rightarrow {}^4B_2$
CoL_4	290	$\pi \rightarrow \pi^*$
	350	$n \rightarrow p^*$
	610	$^4A_1 \rightarrow {}^4B_1$
	690	$^4A_1 \rightarrow {}^4B_2$
CoL_5	260	$\pi \rightarrow \pi^*$
	310	$n \rightarrow p^*$
	590	$^4A_1 \rightarrow {}^4B_1$
	660	$^4A_1 \rightarrow {}^4B_2$
CoL_6	270	$\pi \rightarrow \pi^*$
	390	$n \rightarrow p^*$
	605	$^4A_1 \rightarrow {}^4B_1$
	680	$^4A_1 \rightarrow {}^4B_2$

3.2. Characterization of Metal Complexes

Physical properties of all the synthesized compounds are presented in Table 4. The synthesized metal complexes were prepared in good yield (65–87%), insoluble in ethanol, methanol, chloroform and other common organic solvents but easily soluble in DMSO and DMF. Metal complexes were characterized with mass, Fourier-transform infrared (FT-IR) and Ultraviolet-visible (UV-Visible) spectroscopies. Since the cobalt is paramagnetic in nature the ^{1}H-NMR technique was not performed. The molar conductance values of the complexes in DMSO (10^{-3} M solutions) were calculated at room temperature using $\Lambda_m = \frac{\kappa}{C}$ equation; where C is the concentration of the solutions (mol/L) and κ is

the measured conductivity. Measurements were performed to establish the charge of the complexes. The molar conductivity of the metal complexes lies in the range of 10–22 (Ω^{-1} mol^{-1} cm^2), indicating that all the complexes were non-electrolytes.

Table 4. Physical properties of synthesized compounds. M. W.: molecular weight; M. P.: melting point.

Compounds	M. W. (g/mol)	Yield (%)	Color	Molar Conductivity (Ω^{-1} mol^{-1} cm^2)	M. P. (°C)
L_1	374	84	Dark yellow	-	208–210
L_2	344	86	Orange	-	190–192
L_3	316	64	Brown	-	295–297
L_4	254	68	Yellow	-	203–205
L_5	239	73	Pale Yellow	-	181–183
L_6	225	65	Light green	-	282–284
CoL_1	633	65	Pale green	22	284–250
CoL_2	603	68	Dark green	12	313–315
CoL_3	575	75	Dark brown	14	230–232
CoL_4	503	80	Green	18	280–28
CoL_5	473	82	Orange-red	16	305–307
CoL_6	445	87	Dark-pink	10	236–238

In metal complexes with NO_2 groups (**CoL₁** and **CoL₄**), the NO_2 group can coordinate to the metal center in various ways e.g., via the nitrogen (nitro), oxygen (nitrito), both oxygens (nitrito-*O,O'*) and via nitrogen and oxygen (bridging nitro) [25–27]. The coordination mode of this ambidentate ligand depends on the stereochemical environment around the metal ions. In the FT-IR spectra of **CoL₁** and **CoL₄** complexes the characteristic band in 492 and 614 cm^{-1} is observed which is due to the cobalt-oxygen stretching band; indicating the formation of nitrito isomer. The proposed structure for **CoL₁** and **CoL₄** complexes is given in Figure 2. The band due to ν(C=N) in ligands were shifted to a lower wavenumbers in complexes which indicated the involvement of azomethine group in the coordination to the cobalt center. Also the bands in the range of 1583–1592 cm^{-1} and 1328–1368 cm^{-1} are assigned to the NO_2 groups. In the electronic spectra of **CoL₁** and **CoL₄** complexes the peaks in the range of 600–690 nm are associated with d-d transition; and the low intensity of these peaks indicated the symmetrical structure of these complexes. The mass spectra of these complexes were recorded at room temperature to confirm the stoichiometry of metal chelates as studied above. The molecular ion peak for the **CoL₁** and **CoL₄** complexes were observed at *m/z* = 633 and 573, respectively that are equal to the molecular weight of the complexes.
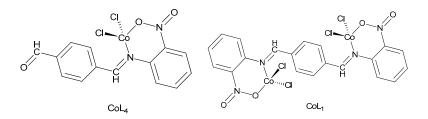

Figure 2. Proposed structure for **CoL₁** and **CoL₄** complexes.

Figure 3 shows the proposed structure for **CoL₂** and **CoL₅** complexes. In FTIR spectra of **CoL₂** and **CoL₅** complexes containing the OMe substituent the (C-H) aliphatic functional groups appeared in the range of 2840–2900 cm^{-1} while the C=NH bands are observed in the range of 1619–1626 cm^{-1}. The peaks in the range of 474–511 cm^{-1} are assigned to the M-O band. The electronic absorption spectrum of **CoL₂** and **CoL₅** complexes showed four peaks. The first and second peaks are due to the π→π* and n→π* transition of ligand group which shifted to higher wavelength compared to free ligand. The d-d transition bands are observed in the range 590–610 and 660–680 nm owing to $^4A_1 \rightarrow ^4B_1$ and $^4A_1 \rightarrow ^4B_2$ transitions. The mass spectra of **CoL₂** and **CoL₅** are in good agreement with the proposed structures. The mass spectra of **CoL₂** and **CoL₅** complexes showed molecular ion peak at *m/z* = 603 and 473, respectively, confirming their formula weight.
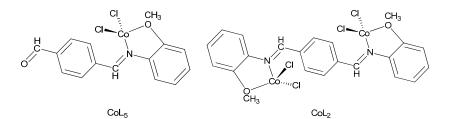
Figure 3. Proposed structure for **CoL₂** and **CoL₅** complexes.

In the FTIR spectra of **CoL₃** and **CoL₆** complexes the stretching frequency of C=N are observed at 1650 and 1634 cm^{-1}, respectively. The disappearance of OH groups in **CoL₃** and **CoL₆** complexes indicate the OH group of ligands has been deprotonated and coordinate to metal ions. The coordination of Schiff base ligands to metals were also proved by the υ (M-O) appearing in the range 485–649 cm^{-1}. The electronic absorption spectra of **CoL₃** and **CoL₆** complexes are very similar to each other. In the UV-Visible spectra of these complexes the π→π* and n→π* transition of ligand group shifted to the higher wavelength upon the coordination and d-d transitions are appeared in the range 600–680 nm. In the mass spectra of **CoL₃** and **CoL₆** complexes the molecular ion peak observed at *m/z* = 575 and 445. The proposed structure for **CoL₃** and **CoL₆** complexes are presented in Figure 4.
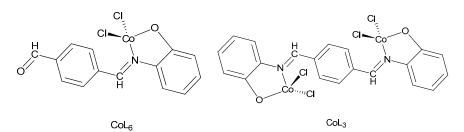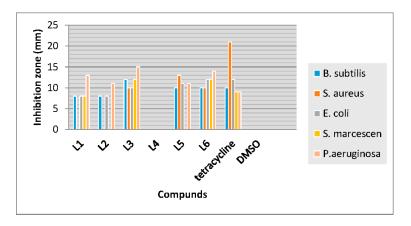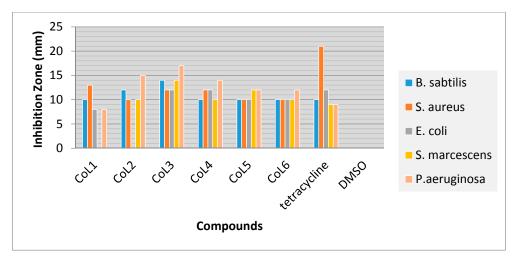

Figure 4. Proposed structure for **CoL₃** and **CoL₆** complexes.

3.3. Antibacterial Activity

Antibacterial activities of the ligands, their metal complexes and standard antibiotic drug (tetracycline) were performed against gram negative bacteria (*Escherichia coli*, *Serratia marcescens* and *Pseudomonas aeruginosa*) and against gram positive bacteria (*Bacillus Subtilis* and *Staphylococcus aureus*) using Muller Hinton agar medium by disk diffusion and broth dilution methods are shown in Figures 5 and 6, respectively.

Figure 5. Graphical presentation of antibacterial activity of ligands against bacterial strains, measuring the inhibition zone (mm). DMSO: dimethyl sulfoxide.

Figure 6. Graphical presentation of antibacterial activity of Co complexes against bacterial strains, measuring the inhibition zone (mm).

From Figure 5 it can be observed that the **L₃** and **L₆** with OH group had relatively higher antibacterial activity compared to the other ligands tested against the bacteria strains. These ligands had better inhibitory effect against *Pseudomonas aeruginosa* with diameter inhibition zone of 15 and 14 mm, respectively. In contrast, the **L₄** with one NO_2 group showed no antibacterial activity against tested bacteria strains.

As can be seen from the antibacterial activity of metal complexes in Figure 6, among all these complexes the **CoL₃** compound showed the higher antibacterial activity with inhibition zone of 14, 12, 12, 14 and 17 mm against *B. Subtilis*, *S. aureus*, *E. coli*, *S. marcescen* and *P. aeruginosa*, respectively. The Minimal Inhibitory Concentration (MIC) values of all the synthesized compounds were also recorded and results are presented in Table 5. From the data listed in Table 5, the MIC values of metal complexes were lower than that of the parent ligands. The antibacterial activities of metal complexes (**CoL₁** to **CoL₆**) against *P. aeruginosa* were more effective than the other tested bacteria strains with MIC value in the range of 0.62 to 2.5 mg/mL. In comparison these metal complexes were less effective against *E. coli*.

Table 5. Minimal inhibitory concentration (mg/mL) ligands and metal complexes based on broth dilution. method.

Compounds	*B. subtils*	*S. aureus*	*E. coli*	*S. marcescen*	*P. aeruginosa*
L₁	2.5	10	5	5	2.5
L₂	2.5	10	2.5	5	2.5
L₃	1.25	5	5	2.5	0.31
L₄	-	-	-	-	-
L₅	2.5	1.25	2.5	5	2.5
L₆	2.5	2.5	2.5	2.5	1.25
CoL₁	1.25	2.5	2.5	2.5	2.5
CoL₂	1.25	5	10	2.5	1.25
CoL₃	0.15	2.5	1.25	0.31	0.15
CoL₄	2.5	1.25	1.25	1.25	0.62
CoL₅	1.25	1.25	1.25	0.62	0.62
CoL₆	1.25	1.25	2.5	1.25	0.62
Tetracycline	5	2.5	5	5	5

It is observed from this study that metal chelates have a higher activity when compared to the parent ligands. Such increased activity of the metal chelates can be explained on the basis of Overtone's concept and chelation theory [28–31]. According to Overtone's concept of cell permeability

the lipid membrane that surrounds the cell favors the passage of only lipid soluble materials due to which liposolubility is an important factor that controls antimicrobial activity. On chelation, the polarity of the metal ion is reduced to a greater extent due to the overlap of the ligand orbital and partial sharing of the positive charge of the metal ion with donor groups. Further, it increases the delocalization of p-electrons over the whole chelate ring and enhances the lipophilicity of the complex. This increased lipophilicity enhances the penetration of the complexes into lipid membranes and blocking of metal binding sites on the enzymes of the microorganism.

4. Conclusions

In this research, we successfully reported the synthesis of the Schiff base ligands (L_1–L_6) and their Co (II) complexes from condensation of Terephthalaldehyde with ortho-anilines with high yields. The synthesis of corresponding ligands was performed under optimized condition. *N*-propyl-benzoguanamine-SO_3H MNPs was used as a suitable catalyst in ethanol as a solvent for the synthesis of the ligands. The structures of the synthesized compounds were proposed by FTIR, ^{1}H-NMR, UV-Vis and mass spectroscopy studies. The molar conductivity measurements showed that all the complexes were non-electrolyte. Antibacterial activities of the ligands and their metal complexes were examined against gram-positive and gram-negative bacteria strains. In general, metal complexes showed much higher antibacterial activities and better inhibitory effects than that of the ligands.

Author Contributions: N.F. conceived and designed the experiments; S.S. performed the experiments and wrote the paper; H.P. analyzed the data, supervised the experiment and contributed reagents/materials/analysis tools and M.D. and F.M. proofing the entire work. All authors read and approved the manuscript.

Conflicts of Interest: The authors declare that there is no conflict of interest.

References

1. Liu, Y.-T.; Sheng, J.; Yin, D.-W.; Xin, H.; Yang, X.-M.; Qiao, Q.-Y.; Yang, Z.-J. Ferrocenyl chaconne-based Schiff bases and their metal complexes: Highly efficient, solvent-free synthesis, characterization, biological research. *J. Organomet. Chem.* **2018**, *856*, 27–33. [CrossRef]

2. Lashanizadegan, M.; Shayegan, S.; Sarkheil, M. Copper(II) complex of (±)trans-1,2-cyclohexanediamine azo-linked Schiff base ligand encapsulated in nanocavity of zeolite-Y for the catalytic oxidation of olefins. *J. Serbian Chem. Soc.* **2016**, *81*, 153–162. [CrossRef]

3. Yu, H.; Zhang, W.; Yu, Q.; Huang, F.-P.; Bian, H.-D.; Liang, H. Ni(II) Complexes with Schiff Base Ligands: Preparation, Characterization, DNA/Protein Interaction and Cytotoxicity Studies. *Molecules* **2017**, *22*, 1772. [CrossRef] [PubMed]

4. Ganguly, R.; Sreenivasulu, B.; Vital, J. Amino acid—Containing reduced Schiff bases as the building blocks for metallasupramolecular structures. *Coord. Chem. Rev.* **2008**, *252*, 1027–1050. [CrossRef]

5. Golcu, A.; Tumer, M.; Demirelli, H.; Wheatley, R.A. Cd and Cu complexes of polydentate Schiff base ligands: Synthesis, characterization, properties and biological activity. *Inorg. Chim. Acta* **2005**, *153*, 1785–1797. [CrossRef]

6. Sarkar, S.; Jana, M.; Mondal, T.; Sinha, C. Ru-halide-carbonyl complexes of naphthylazoimidazoles; synthesis, spectra, electrochemistry, catalytic and electronic structure. *J. Organomet. Chem.* **2012**, *716*, 129–137. [CrossRef]

7. Khandar, A.; Nejati, K.; Rezvani, Z. Syntesis, characterization, and study of the use of cobalt Schiff base complexes as catalysts for the oxidation of styrene by molecular oxygen. *Molecules* **2005**, *10*, 302–311. [CrossRef] [PubMed]

8. Raman, N.; Ravichandran, S.; Thangaraja, C. Copper, Cobalt, Nickel and zink complexes of Schiff base derived from benzil-2,4-dinitrophenylhydrazone wiyh aniline. *J. Chem. Sci.* **2004**, *116*, 215–219. [CrossRef]

9.   Al Zoubi, W.; Ko, Y.G. Schiff base complexes and their versatile applications as catalysts in oxidation of organic compounds: Part I. *Appl. Organomet. Chem.* **2016**, *31*. [CrossRef]

10.   Siva, C.; Silva, D.; Modolo, L.; Alves, R.; Rwsende, M.; Martins, C.; Fatima, A. Schiff bases: A short review of their antimicrobial activities. *J. Adv. Res.* **2011**, *2*, 1–8. [CrossRef]

11.   Afradi, M.; Foroughifar, N.; Psdar, H.; Moghhanian, H. Facile green one-pot synthesis of novel thiazolo[3,2-a]pyrimidine derivatives using Fe_3O_4 L-argainine and their biological investigation as potent antimicrobial agents. *Appl. Organomet. Chem.* **2016**, 1–16. [CrossRef]

12.   Anitha, C.; Sheela, C.; Tharmaraj, P.; Sumathi, S. Spectroscopic studies and biological evaluation of some transition metal complexses of azo schiff base ligand derived from (1-phenyl-2,3-dimethyl-4-aminopyrazol-5-one) and 5-((4-chlorophenyl)diazenyl)-2-hydroxybenzaldehyde. *Spectrochim. Acta Part A* **2002**, *96*, 493–900. [CrossRef] [PubMed]

13.   Raman, N.; Raja, Y.P.; Kulandaisamy, A. Synthesis and characterisation of Cu(II), Ni(II), Mn(II), Zn(II) and VO(II) Schiff base complexes derived fromo-phenylenediamine and acetoacetanilide. *J. Chem. Sci.* **2001**, *113*, 183–189. [CrossRef]

14.   Raman, N.; Thangaraja, C.; Johnsonraja, S. Synthesis, spectral characterization, redox and antimicrobial activity of Schiff base transition metal(II) complexes derived from 4-aminoantipyrine and 3-salicylideneacetylacetone. *Cent. Eur. J. Chem.* **2005**, *3*, 537–555. [CrossRef]

15.   Streater, M.; Taylor, P.D.; Hider, R.C.; Porter, J. Novel 3-hydroxyl-2(1H)-pyridinones. Synthesis, iron(III)-chelating properties and biological activity. *J. Med. Chem.* **1990**, *33*, 1749–1755. [CrossRef] [PubMed]

16.   Abdel-Latif, S.A.; Hassib, H.B.; Issa, Y.M. Studies on some salycylaldehyde schiff base derivatives and their complexes with Cr, Mn, Ni, Cu. *Spectrochim. Acta Part A* **2007**, *67*, 950–957. [CrossRef] [PubMed]

17.   Lo, K.; Cornell, H.; Nicoletti, G.; Jackson, N.; Hügel, H. Study of Fluorinated β-Nitrostyrenes as Antimicrobial Agents. *Appl. Sci.* **2012**, *2*, 114–128. [CrossRef]

18.   Tolazzal, M.; Tarafder, H.; Ali, M.; Juan, D. Complexes of a tridentate ONS Schiff base. Synthesis and biological properties. *Transit. Metal Chem.* **2000**, *25*, 456–460. [CrossRef]

19.   Khojasteh, R.; Matin, S.J. Synthesis, characterization and antimicrobial activity of some metal complexes of heptadentate schiif base ligand derived from acetylacetone. *Russ. J. Appl. Chem.* **2015**, *88*, 921–925. [CrossRef]

20.   Hou, S.H.; Jihui, J.; Huang, X.; Wang, X.; Ma, L.; Shen, W.; Kang, F.; Hiang, Z.-H. Silver Nanoparticles-Loaded Exfoliated Graphite and Its Anti-Bacterial Performance. *Appl. Sci.* **2017**, *7*, 852. [CrossRef]

21.   Lee, J.; Purushothaman, B.; Li, Z.; Kulsi, G.; Song, J.M. Synthesis, Characterization, and Antibacterial Activities of High-Valence Silver Propamidine Nanoparticles. *Appl. Sci.* **2017**, *7*, 736. [CrossRef]

22.   Wang, S.X.; Zhang, F.J.; Feng, Q.P.; Li, Y.L. Synthesis, characterization, and antibacterial activity of transition metal complexes with 5-hydroxy-7,4′-dimethoxyflavone. *J. Inorg. Biochem.* **1992**, *46*, 251–257. [CrossRef]

23.   Gholami Dehbalaei, M.; Foroughifar, N.; Pasdar, H.; Khajeh-Amiri, A. *N*-Propyl benzoguanamine sulfonic acid supported on magnetic Fe_3O_4 nanoparticles: A novel and efficient magnetically heterogeneous catalyst for the synthesis of 1,8-dioxo-decahydroacridine derivatives. *New J. Chem.* **2018**, *42*, 327–335. [CrossRef]

24.   Camus, A.; Marsich, N.; Lanfredi, A.M.M.; Ugozzoli, F.; Massera, C. Copper(II) nitrito complexes with 2,20-dipyridylamine. Crystal structures of the [(acetato)(2,20-dipyridylamine)(nitrito-O,O0)copper(II)] and [(2,20-dipyridylamine) (nitrito-O,O0)(_-nitrito-O)copper(II)]2_2(acetonitrile). *Inorg. Chim. Acta* **2000**, *309*, 1–9. [CrossRef]

25.   Mautner, F.A.; Vicente, R.; Massoud, S.S. Structure determination of nitrito- and thiocyanato-copper(II) complexes: X-ray structures of [Cu(Medpt)(ONO)(H_2O)]ClO_4(1), [Cu(dien)(ONO)]ClO_4 (2) and [Cu_2(Medpt)_2(_N,S-NCS)_2](ClO4)_2 (3) (Medpt = 3,30-diamino-*N*-methyldipropylamine and dien = diethylenetriamine). *Polyhedron* **2006**, *25*, 1673–1680. [CrossRef]

26.   Eslami, A. Thermoanalytical study of linkage isomerism in coordination compounds: Part I. Reinvestigation of thermodynamic and thermokinetic of solid state interconversion of nitrito (ONO) and nitro (NO_2) isomers of pentaaminecobalt(III) chloride by means of DSC. *Thermochim. Acta* **2004**, *409*, 189–193. [CrossRef]

27.   Pasdar, H.; Hedayati Saghavaz, B.; Foroughifar, N.; Davallo, M. Synthesis, Characterization and Antibacterial Activity of Novel 1,3-Diethyl-1,3-bis(4-nitrophenyl)urea and Its Metal(II) Complexes. *Molecules* **2017**, *22*, 2125. [CrossRef] [PubMed]

28.   El-Megharbel, S.M.; Adam, A.M.; Meghdad, A.S.; Refat, M.S. Synthesis and molecular structure of moxifloxacin drug with metal ions as amodel drug against some kinds of bacteria and fungi. *Russ. J. Gen. Chem.* **2015**, *85*, 2366–2371. [CrossRef]

29. Patel, M.N.; Pansuriya, P.B.; Parmar, P.A.; Gandhi, D.S. Synthesis, characterization and thermal and biocidal aspects of drug-based metal complexes. *Pharm. Chem. J.* **2008**, *42*, 687–692. [CrossRef]

30. Hedayati Saghavaz, B.; Pasdar, H.; Foroughifar, N. Novel dinuclear metal complexes of guanidine-pyridine hybrid ligand: Synthesis, structural characterization and biological activity. *Biointerface Res. Appl. Chem.* **2016**, *6*, 1842–1846.

31. Khadivi, R.; Pasdar, H.; Foroughifar, N.; Davallo, M. Synthesis and structural characterization of metal complexes derived from substituted guanidine-pyridine as potential antibacterial agents. *Biointerface Res. Appl. Chem.* **2017**, *7*, 2238–2242.